Evaluation of the Phase-Aggression Criterion for PIO Detection in Real-Time

Simone Fasiello
Ph.D. Student
University of Liverpool
Liverpool, United Kingdom
and
Politecnico di Milano
Milan, Italy

Michael Jump
Senior Lecturer
University of Liverpool
Liverpool, United Kingdom

Pierangelo Masarati
Professor
Politecnico di Milano
Milan, Italy

ABSTRACT

This paper presents the results of a pilot-in-the-loop experiment performed to investigate the efficacy of a pilot-induced oscillation (PIO) or adverse rotorcraft-pilot coupling (RPC) real-time detection method, to be implemented as an in-cockpit warning system. A test pilot performed a number of simulated flights inside the Heliflight-R simulator at the University of Liverpool. Two handling qualities (HQ) mission task element (MTE) maneuvers were chosen, namely Precision Hover and Lateral Reposition. The baseline dynamics were those of a FLIGHTLAB BO105-like helicopter model, as used in previous tests; changes in rate limits were introduced to induce the pilot-vehicle system (PVS) to be more RPC/PIO prone, and to observe pilot's adaptation to these variations causing system instabilities during the chosen MTEs. To objectively measure the severity of the PIO encountered during the tests, the Phase-Aggression Criterion (PAC) has been used. This method has been developed to allow for real-time PIO detection in order to provide the information inside the cockpit. In addition, pilot subjective ratings were collected, by using the HQs, PIO and Pilot Workload rating scales. Overall, the results show a good correlation between objective and subjective evaluations, and that it is possible to detect PIOs in real-time. The information can be provided to the pilot by means of visual, aural or haptic cues, which is the work the authors are currently carrying out.

NOTATION

A_G	Aggression, deg/s^2
H_s	Control Gearing, $(deg/s)/in$
p	Roll rate, deg/s
q	Pitch rate, deg/s
$T_{\delta_{PK_1}}$	Time of last control peak, s
$T_{\delta_{PK_2}}$	Time of current control peak, s
$T_{q_{PK_1}}$	Time of last pitch rate peak, s
$T_{q_{PK_2}}$	Time of current pitch rate peak, s
$T_{p_{PK_1}}$	Time of last roll rate peak, s
$T_{p_{PK_2}}$	Time of current roll rate peak, s
Φ	Phase delay, deg
$\delta_{\theta_{1c}}$	Lateral cyclic control, in
$\delta_{\theta_{1s}}$	Longitudinal cyclic control, in
θ_{1c}	Lateral swashplate deflection, deg
θ_{1s}	Longitudinal swashplate deflection, deg

INTRODUCTION

Rotorcraft-Pilot Couplings (RPCs) are defined as undesirable phenomena originating from an anomalous interaction between pilot and rotorcraft [1–3]. The term RPC includes any kind of unfavorable event related to involuntary unstable rotorcraft responses resulting from pilot control actions within the control loop, whether they are active or passive, oscillatory or non-oscillatory. The most common or well-known form of RPC is a Pilot-Induced Oscillation (PIO). The term PIO refers specifically to an oscillatory aircraft response, characterized by an 'active' pilot trying to control the vehicle within the control loop, which inadvertently excites self-sustained and potentially divergent vehicle oscillations.

This work, carried out within the NITROS[2] Project, aims to develop and evaluate a toolset able to *detect PIOs in (near) real-time* in modern rotorcraft, as well as *alleviating* the unwanted event if it occurs. In this paper, the first of these aspects, i.e. detection, is studied by inspection of flight simulation data available at the University of Liverpool. The intent initially is to use this information to design an alert system, which will be used to provide the pilot with visual cues to enable him/her to suppress a PIO as it starts developing (i.e. a form of manual alleviation).

Previous work at the University of Liverpool focused on a means to identify PIO events offline, after they had occurred. This led to the development of the Phase-Aggression Criterion (PAC) [4, 5]. For this investigation, PAC has been developed further to support near real-time data acquisition and PIO detection. The detection is 'near' to real time as a number of data samples have to be taken to perform the detection. The detection therefore lags real-time by the sampling period.

One of the first tools developed to detect PIOs in real-time is the Real-time Oscillation Verifier (ROVER) [6–

[1]Presented at the Vertical Flight Society's 77th Annual Forum & Technology Display, Virtual, May 10-14, 2021.

[2] NITROS: NITROS: Network for Innovative Training on Rotorcraft Safety - https://www.nitros-ejd.org

8]. This study makes use of ROVER, as a comparator to the real-time PAC method.

This paper is structured as follows. In the next Section PAC is briefly described in its post-processing detection form, along with the associated PAC chart and PIO severity regions. Next, the real-time detection version of PAC is presented, and comparisons between the ROVER and PAC detection methods are presented. The experimental setup and procedure (MTEs, experimental conditions, warning system) used in the paper is then described. The results of these experiments are shown in terms of subjective and objective evaluations. Finally, the paper ends with a brief Discussion and some Conclusions.

METHOD

This Section presents PAC as a post-processing detection method and the usefulness of its associated detection boundaries.

Background

PAC was designed at the University of Liverpool, during the EC-FP7 program ARISTOTEL[3] as a post-processing tool (hereafter, PP-PAC) to objectively verify the presence of PIOs during piloted simulation test campaigns. Being aware of the importance of pilot opinion, the simulation results in Ref. [5] were supported by pilot subjective ratings collected using two rating scales: the PIO Tendency Rating Scale (PIOR) defined in Refs. [9–11] and the Adverse Pilot Couplings Scale (APCS) [4]. The latter was developed in response to the perceived deficiencies of the former, such as descriptor inconsistencies, and providing little information about the severity of the PIO itself.

A key element of the PAC method is the PAC Chart (Figure 1). The PAC chart consists of three regions which distinguish between the different PIO severities based upon Phase Delay and pilot Aggression. For a more complete treatment of the PAC algorithm and severity regions, the reader is referred to Ref. [4].

Offline Detection Method PP-PAC

The PAC method drew its inspiration from Pilot-Inceptor Workload (PIW) theory [12, 13]. PIW focuses on the pilot input through the use of the Duty Cycle (measure of pilot activity) and the Aggression (A_G measure of magnitude and rate of control inputs). PAC extended PIW theory by taking into account information regarding the vehicle dynamics and output, i.e. the Phase Delay (Φ between pilot input and aircraft output), in order to observe PIOs that occurred during the flight. A_G is a measure of the pilot control activity, i.e. how intensively the pilot is working to achieve the task. The faster and/or larger the control input, the higher the A_G. The Φ indicates the phase delay between pilot input and aircraft response (e.g. $\Phi = 90\ deg$ means aircraft response out of phase with respect to the pilot input).

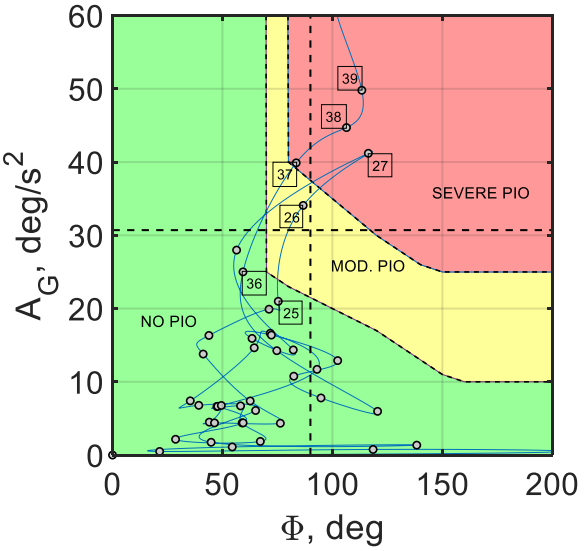

Figure 1. PAC Chart example showing the PIO severity boundaries (Green = No PIO, Yellow = Moderate PIO, Red = Severe PIO), data points with rounded time stamp and interpolation

Figure 2 shows an example of a time-history, which portrays pilot input in black and rotorcraft angular rate in red for the longitudinal axis. These are used for the calculation of the PAC parameters Φ and A_G. These two terms are expressed, for the longitudinal axis, in Equations (1) and (2):

$$\Phi = 360° \frac{T_{q_{PK_2}} - T_{\delta_{PK_2}}}{T_{q_{PK_2}} - T_{q_{PK_1}}}; \quad (1)$$

$$A_G = \frac{H_s}{T_{q_{PK_2}} - T_{q_{PK_1}}} \int_{T_{q_{PK_1}}}^{T_{q_{PK_2}}} \left|\dot{\delta}_{\theta_{1s}}(t)\right| dt; \quad (2)$$

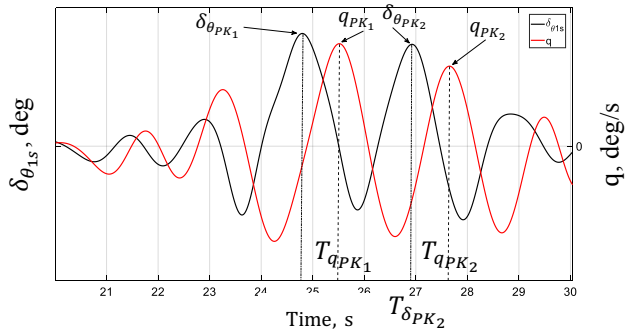

Figure 2. Example of the section of a time history for the PAC calculations

where $T_{q_{PK_1}}$, $T_{q_{PK_2}}$ and $T_{\delta_{PK_2}}$ represent the time at the beginning of the current oscillation cycle (first rate peak detected during the cycle), the time at the end of the current

[3] ARISTOTEL: Aircraft and Rotorcraft Pilot Couplings: Tools and Techniques for Alleviation and Detection, http://www.aristotel-project.eu/

oscillation cycle (second rate peak detected) and the time of the input peak detected during the cycle respectively. The H_s term, for PP-PAC, represents the average control gearing, i.e. the ratio of rotorcraft output (rotational rate) to pilot control input over the entire response. This term was introduced to allow PAC to be applied to different rotorcraft. In the PAC definition work, a rotorcraft model based upon the BO105, which has a rate command (RC) response type, was used. The units of A_G are, in this case, therefore, deg/s^2.

Real-time Detection Method

The large amount of useful data that was collected during the ARISTOTEL test campaigns, has been inspected to develop a real-time detection and alerting system using the Phase-Aggression Criterion (RT-PAC). Therefore, PAC has been implemented within the Heliflight-R simulation facility [14] in order to provide real-time warnings to the pilot. The primary focus of the NITROS test campaign described in this paper is indeed to develop and evaluate a toolset able to detect RPC/PIOs in (near) real-time in modern rotorcraft, as well as facilitating the pilot in alleviating the unwanted event if it occurs. In this Subsection, the importance of the control gearing term is highlighted, the real-time version of PAC (RT-PAC) is described with a case study using flight simulation data, and the idea behind the warning system is presented.

CONTROL GEARING

The control gearing, H_s, plays a crucial role, because it is the term that most influences the magnitude of A_G. In PP-PAC, H_s was calculated as the mean value of the ratio between output and input for the whole manoeuvre of interest. This is acceptable for the post-processing analysis, for which it was originally intended, but it is not useful for the calculation of A_G in real-time. To remedy this, a steady state value of H_s has been used for RT-PAC. It is calculated to be the ratio between the steady-state values of rotorcraft rates and pilot cyclic controls for a step input in the axis of interest, as shown in Equation 3.

$$H_{s_{long}} = \frac{\Delta q}{\Delta \delta_{\theta_{1s}}} = \frac{\theta_{1s}}{\Delta \delta_{\theta_{1s}}} \frac{\Delta q}{\theta_{1s}}; \quad (3.1)$$

$$H_{s_{lat}} = \frac{\Delta p}{\Delta \delta_{\theta_{1c}}} = \frac{\theta_{1c}}{\Delta \delta_{\theta_{1c}}} \frac{\Delta p}{\theta_{1c}}; \quad (3.2)$$

CASE STUDY

To demonstrate how RT-PAC performs in comparison to PP-PAC, the following case study is considered. The data comes from flight simulation data, where the ADS-33 Precision Hover maneuver was performed using a BO105-'like' nonlinear model [4]. Time delays and rate limits were added to the helicopter control system in the longitudinal and lateral axes to trigger PIOs. Figure 3(a) shows the time-history of pilot control input (black line) and rotorcraft rate response (grey dashed line), in the longitudinal axis only, of a case in which PIOs were encountered during the tests. Clearly, sustained oscillations occurred during this run, between approximately t = 18 and 38 seconds and then again between t = 63 and 87 seconds. To assess whether there are significant differences between the outputs of the methods, the case study data have also been used to perform a comparison between ROVER, PP-PAC and RT-PAC. Figures 3(b), (c) and (d) show the ROVER, PP-PAC and RT-PAC scores respectively, representative of the PIO detection and severity. For the PAC analysis, a score of 1 represents a moderate PIO and a score of 2 a severe PIO. All methods detect PIOs in approximately the same time intervals, i.e. between t = 18 and 38 seconds, t = 63 and 72 seconds and t = 85 and 87 seconds. These results are quite encouraging. Each method gives reasonably similar detection percentages, and do so in a correlated way along the time history.

Figure 4 shows the corresponding RT-PAC chart. As previously mentioned, due to the different H_s used, in the y-axis, the aggression values are the same in character but somewhat different in the detail in the RT-PAC chart than in the PP-PAC one (not shown here).

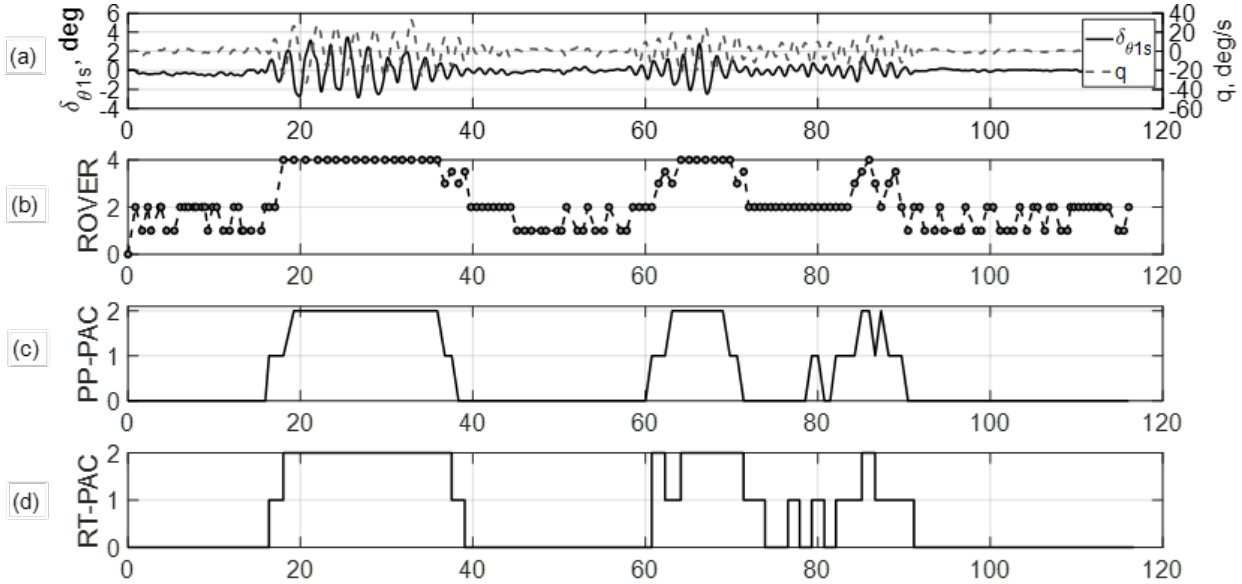

Figure 3. Time history and comparison between ROVER and PAC detection

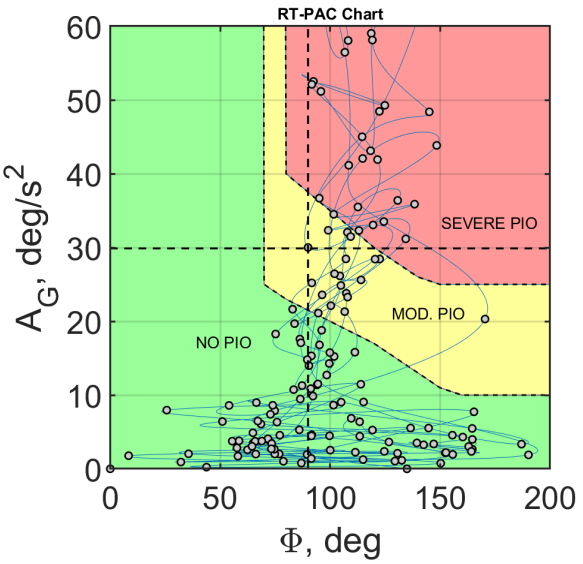

Figure 4. Real-time PAC chart

WARNING SYSTEM

The intent is to use a warning system to provide the pilot with a set of cues to enable him/her to suppress a PIO either before or as it happens (i.e. a form of manual alleviation). As a start point for this research, a traffic light-style head-up display symbol set was developed to advise the pilot by means of visual cues as soon as a PIO is detected by the algorithm in use. The display is situated in the visual field in such a way that it does not interfere with the pilot's ability to perform the primary task. For a NO PIO situation, the display indicates no color. When moderate and severe PIOs are detected, the display indicates yellow and red respectively. The expectation is that the display will indicate to the pilot that a PIO is in progress such that a control strategy can be adopted to suppress it. Given that PIOs usually happen during tasks which require a high pilot control gain, one solution might be for the pilot to 'reduce his/her gain', but, for the present paper, the choice of alleviation strategy is left to the pilot. Further details about the warning system can be found in the next Section, in the dedicated Display Subsection.

TEST CAMPAIGN AND EXPERIMENTAL SET-UP

The following Section discusses the test campaign that took place in the Heliflight-R (see Figure 5) simulator at the University of Liverpool, and the experimental set-up in further detail.

The test campaign was conducted using a single former test pilot, with experience in providing subjective opinion ratings and overall assessment of vehicle handling qualities. The test pilot had also participated in some of the ARISTOTEL test campaigns and was therefore familiar with the processes involved. He also had had extensive experience in using the Heliflight-R simulator. The baseline rotorcraft dynamics used was the one of a BO105-like FLIGHTLAB model [4].

Figure 5. Heliflight-R, University of Liverpool

Mission Task Elements

In the ARISTOTEL test campaigns, some insight was obtained with respect to maneuver suitability to promote RPCs when necessary. This included considerations for the overall task suitability in relation to the simulation device used. For instance, in the Heliflight-R, low speed maneuvers showed high potential to expose RPCs. Based on experience from the ARISTOTEL test campaigns, two maneuvers have been selected for further investigation: Precision Hover (PH) and Lateral Reposition (LR). The maneuver descriptions are reported in Table 1.

Table 1. Mission Task Elements

MTE	Axis	Description
Precision Hover	Lateral and Longitudinal	Test RT-PAC detection in the longitudinal and lateral axes, for Cat. I and Cat. II PIOs. PIO incipience through changes in the rate limits.
Lateral Reposition	Lateral and Longitudinal	Test the RT-PAC detection mainly in the lateral axis, for Cat. I and Cat. II PIOs. Detection kept active also in the longitudinal axis.

The Precision Hover and Lateral Reposition MTEs will be further detailed in the next Subsections.

PRECISION HOVER

The Precision Hover maneuver is initiated with the aircraft travelling at a ground speed of between 6 and 10 knots, at an altitude of less than 20 feet. The target hover point is to be oriented at 45° relative to the heading of the rotorcraft. The ground track should be such that the rotorcraft will arrive over the target hover point. The hover should be captured in one smooth maneuver following the initiation of deceleration – it is not acceptable to accomplish most of the deceleration well before the hover point and then to "creep up" to the final position. Figure 6 and Table 2 show the test course and the performance standards for this MTE.

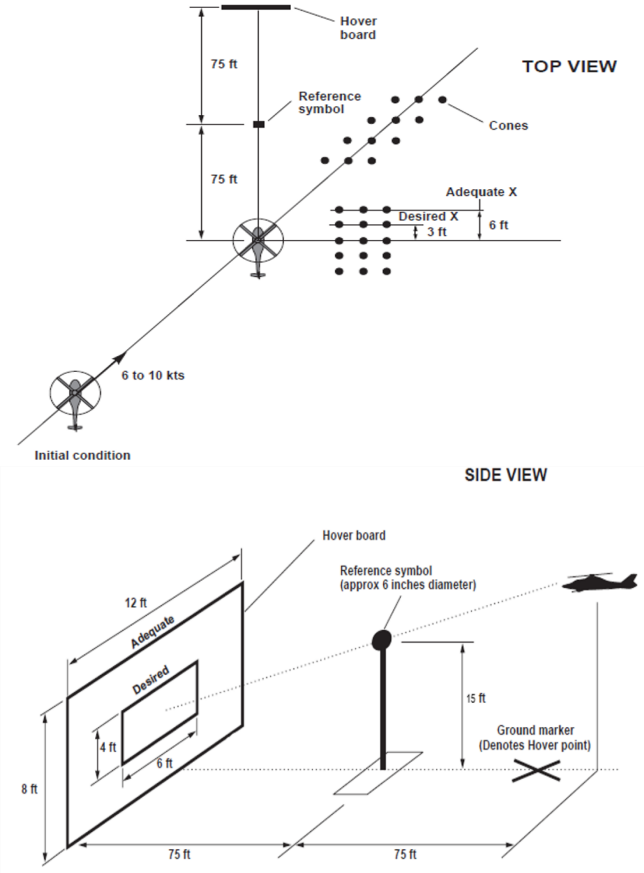

Figure 6. Top View and Side View of the Precision Hover MTE

Table 2. Precision Hover Performance Requirements

Performance	Desired	Adequate
Attain stabilized hover within X seconds of initiation of deceleration	5	8
Maintain a stabilized hover for at least X seconds	30	30
Maintain the longitudinal and lateral position within ±X feet on the ground	3	6
Maintain altitude within ±X feet	2	4
Maintain heading within ±X °	5	10

LATERAL REPOSITION

The lateral reposition is a MTE for assessing the lateral HQs of a rotorcraft and is a high aggression maneuver. The task is to accelerate the rotorcraft to a certain target airspeed that allows the lateral reposition to be completed within 18 seconds. The second phase requires deceleration back to a stabilized hover at the marked end point (450 ft from the start). Figure 7 shows the test course schematic.

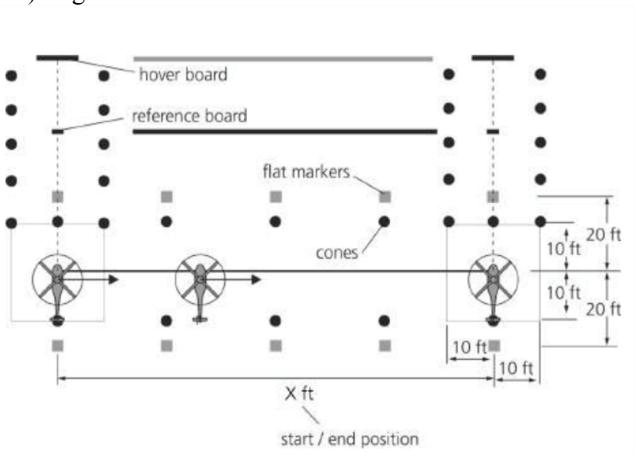

Figure 7. Top View of the Lateral Reposition MTE

Table 3 shows the performance standards for this MTE.

Table 3. Lateral Reposition Performance Requirements

Performance	Desired	Adequate
Maintain altitude within ±X feet	10	15
Maintain longitudinal track within ±X feet	10	20
Maintain heading within ±X °	10	15
Complete manoeuvre within X seconds	18	22

Experimental Conditions

The majority of maneuvers conducted within the ARISTOTEL test campaigns were performed using time delays and rate limits specifically designed to make the system prone to pilot-vehicle instability. Tests conducted with rate limits were found to be more successful within Heliflight-R, causing severe RPCs during Precision Hover, Roll Step, Pitch Tracking and Acceleration-Deceleration manoeuvres. For this reason, different values of rate limiters have been applied to "trigger PIOs" during the test campaign reported in this paper. Table 4 shows the selection of the experimental conditions. Indeed, in this experiment different settings of lateral and longitudinal rate limits were chosen and tested. It would be expected that these variations, with respect to the baseline configuration C0, will result in more degraded control characteristics possibly causing undesirable and unintentional vehicle responses, resulting in sustained severe oscillations, i.e. PIOs.

Table 4. Experimental Conditions

Configuration	Lateral RL (deg/s)	Longitudinal RL (deg/s)
C0	-	-
C1	2.5	-
C2	3.6	3.6
C3	2.5	5
C4	2.5	2.5
C5	1.8	3.6
C6	1.8	1.8
C7	1.25	2.5

Display

As mentioned in the previous Section, a display was provided to the pilot, showing information about the severity of any PIO detected in near real-time.

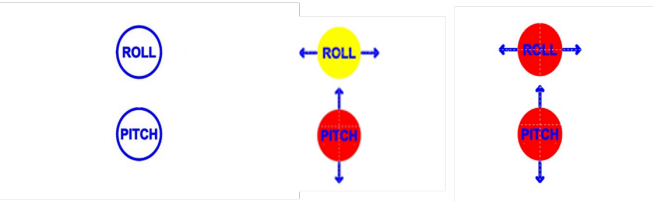

Figure 8. Traffic light Display, for lateral and longitudinal PIO detection

The head-up display is composed of a set of two traffic light displays, one representing the PIO detection in the lateral (roll) axis and one representing the PIO detection in the longitudinal (pitch) axis. Figure 8 illustrates three different hypothetical cases of the same display. The case on the left side represents a "NO PIO" situation in both axes, the case in the middle represents a situation in which a moderate PIO and a severe PIO have been detected in the lateral and longitudinal axis respectively, the case on the right side represents a situation in which a severe PIO has been detected in both axes. When either of the displays indicates 'yellow', it means that the pilot has entered a moderate PIO situation. This is a first stage of the alert process, meaning that, by not changing strategy (e.g. keeping high the control activity), the pilot may enter severe PIO situations, leading to even more critical scenarios, indicated by the display turning 'red'. Furthermore, to aid pilot attention getting qualities of the display, the arrows (indicating the axis where the PIO is occurring) are displayed only in the case when the PIO has been detected.

RESULTS

Pilot's Subjective Ratings

The assessment of HQ, PIO and workload tendencies was completed through use of subjective opinion scales. The pilot was asked to award Cooper-Harper Handling Qualities Ratings (HQR) [15], PIO ratings using both the PIO Tendency Rating scale (PIOR) [9, 11] and the Adverse Pilot Couplings Scale (APCS) [4], and Bedford Workload ratings [16]. For simplicity, the PIO tendencies assessment will be done only through the APCS in this Section.

Figure 9 shows the pilot's subjective ratings collected during the trial for the Precision Hover maneuver: the black square, the red triangle, and the blue circle indicate the HQRs, the Adverse Pilot Coupling, and the Bedford Workload ratings, respectively. On the x-axis, the different configurations are reported, in terms of rate limits variation (see Table 4 for reference) selected in the lateral and longitudinal axes during the trial.

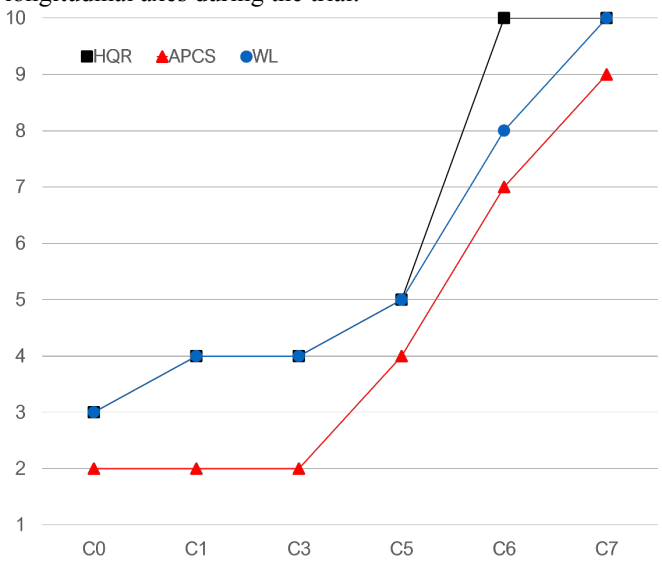

Figure 9. Subjective Ratings against Configurations tested for Precision Hover

Going from the baseline configuration C0 to C1 or C3 leads to a slight increase of HQR (from 3 to 4, therefore from Level 1 satisfactory to Level 2 acceptable but unsatisfactory HQs) and pilot workload; no PIO was perceived by the pilot (APCS=2). Unexpectedly, there is no change in subjective ratings between C1 and C3 (meaning that adding a rate limit of 5 deg/s in the longitudinal axis did not make a difference for the pilot during Precision Hover). It is interesting to notice that, when moving from C5 to C6 (i.e. when changing the longitudinal rate limit from 3.6 to 1.8 deg/s, while the lateral rate limit is 1.8 deg/s for both configurations), there is a significant degradation in performance, with a consequent increase in all ratings: HQR=10, APCS=7E and WL=8, as well as when selecting C7 (configuration in which the rate limit is the lowest, 1.25 deg/s in the lateral axis): HQR=10, APCS=9E, WL=10, which means severe oscillations forcing the pilot to abandon the task. This is an indication of the fact that, with the selected configurations within the Precision Hover maneuver, the pilot entered PIO situations and crossed the moderate-severe PAC boundaries.

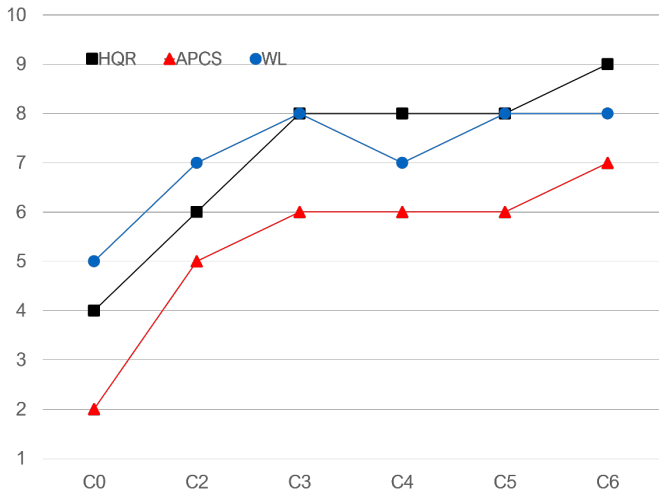

Figure 10. Subjective Ratings against Configurations tested for Lateral Reposition

Figure 10 shows the pilot's subjective ratings collected during the experiment for the Lateral Reposition maneuver: similarly, the black square, the red triangle, and the blue circle indicate the HQRs, the Adverse Pilot Coupling, and the Bedford Workload ratings, respectively. In this case, the degradation of performance, with respect to the baseline configuration C0, is already visible for C2 and C3 (configurations in which the rate limits are 3.6 deg/s in the longitudinal axis and 2.5 deg/s in the lateral axis). This is an indication that the PVS may be more PIO prone during Lateral Reposition than Precision Hover, probably because the Lateral Reposition task required a quicker completion leading the pilot to use higher rates that were eventually limited. For C3 the pilot awarded: HQR=8, APCS=6B, WL=8, very similar to the ratings awarded for C4 and C5: HQR=8, APCS=6D, WL=8. In both cases pilot adaptation was necessary, the main difference between C3 and C4-C5 is that an APCS rating of 6B means sustained severe convergent oscillations, 6D means divergent severe oscillations. Curiously, the Workload rating goes from 8 to 7 from C3 to C4 (case in which the longitudinal rate limit was reduced from 5 to 2.5 deg/s), which is the opposite of what was expected; this would usually be due to the pilot getting better in the task leading to a lower Workload rating, but in this case it was most probably due to pilot's fatigue leading to a higher Workload rating (given that C3, the configuration in which the longitudinal rate limit was 5 deg/s, took place towards the end of the test campaign, after C4, the one in which it was 2.5 deg/s). Finally, as expected, C6 is the configuration leading to very poor performance within the Lateral Reposition maneuver: HQR=9, APCS=7D and WL=8, meaning that the pilot encountered severe divergent vehicle oscillations which required high level of adaptation and consumed the majority of workload.

Real-time Detection and Objective Evaluation

In this Subsection, the main results in terms of "objective" RT-PAC detection will be reported.

First of all, Tables 5 and 6 present a summary of the subjective ratings and detection percentages of the whole set of configurations tested for Precision Hover and Lateral Reposition. The columns relative to the lateral and longitudinal detection percentages report three values representative of the time percentages in which no PIOs, moderate PIOs and severe PIOs were detected. There seem to be a good correlation between the pilot's subjective ratings and the objective PAC detection percentages.

Table 5. Precision Hover Results

Conf.	HQ	WL	APCS	PIO	Lat PAC %	Long PAC %
C0	3	3	2	2	99-1-0	86-8-6
C1	4	4	2	2	92-8-0	95-5-0
C3	4	4	2	2	93-7-0	97-3-0
C5	5	5	4B	3	81-13-6	96-1-3
C6	10	8	7E	6	65-27-8	62-26-12
C7	10	10	9E	6	50-27-23	51-21-28

Table 6. Lateral Reposition Results

Conf.	HQ	WL	APCS	PIO	Lat PAC %	Long PAC %
C0	4	5	2	2	100-0-0	76-24-0
C2	6	7	5B	4	70-30-0	73-18-9
C3	8	8	6B	4	40-55-5	92-8-0
C4	8	7	6D	4	58-23-19	70-23-7
C5	8	8	6D	4	52-46-2	72-19-9
C6	9	8	7D	4	46-34-20	25-60-15

For the sake of simplicity, only the results of one configuration for each MTE along one axis will be reported. Figures 11, 12, 13 and 14 show the time history of lateral control input, roll rate response and swashplate deflection, the real-time PAC detection and the PAC chart for the Precision Hover maneuver performed with C7.

A good number of moderate and severe PIOs have been detected for C7 through the Precision Hover maneuver, precisely for 27% and 23% of the time history, respectively.

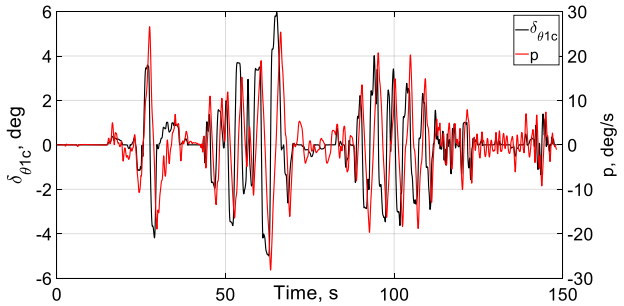

Figure 11. Time history of Lateral Control Input and Rotorcraft Rate Response, C7, PH

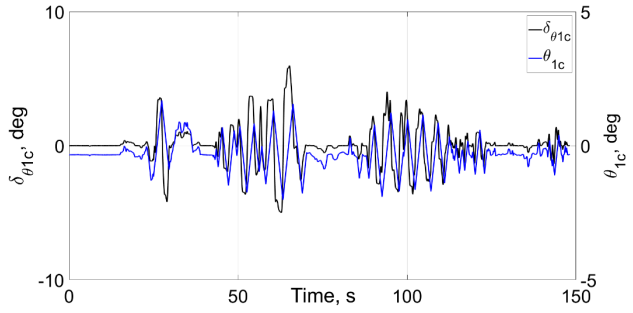

Figure 12. Time history of Lateral Control Input and Swashplate Deflection, C7, PH

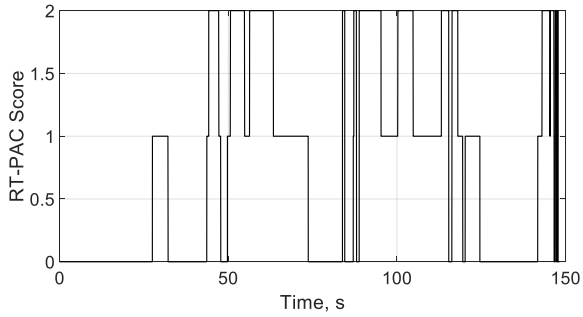

Figure 13. RT-PAC Detection, C7, PH

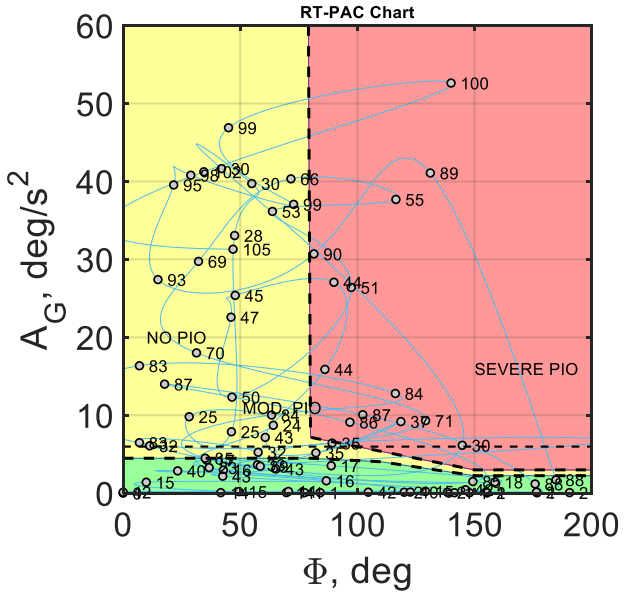

Figure 14. RT-PAC Chart, C7, PH

Figures 15, 16, 17 and 18 show the time history of lateral control input, roll rate response and swashplate deflection, the real-time PAC detection and the PAC chart for the Lateral Reposition maneuver performed with C4.

Also in this case a good number of moderate and severe PIOs have been detected for C4 through the Lateral Reposition maneuver, precisely for 23% and 19% of the time history, respectively.

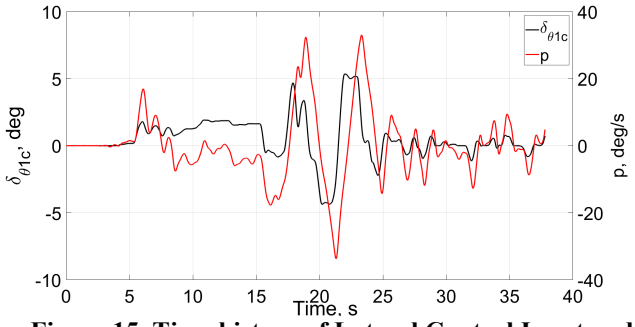

Figure 15. Time history of Lateral Control Input and Rotorcraft Rate Response, C4, LR

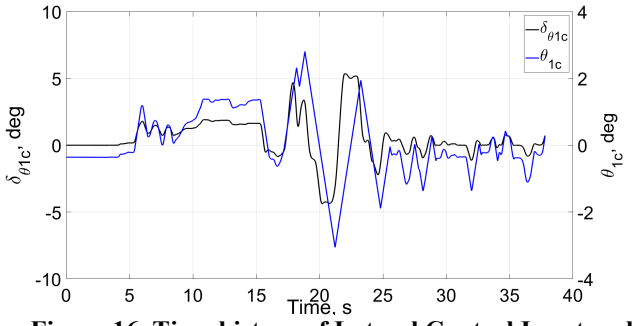

Figure 16. Time history of Lateral Control Input and Swashplate Deflection, C4, LR

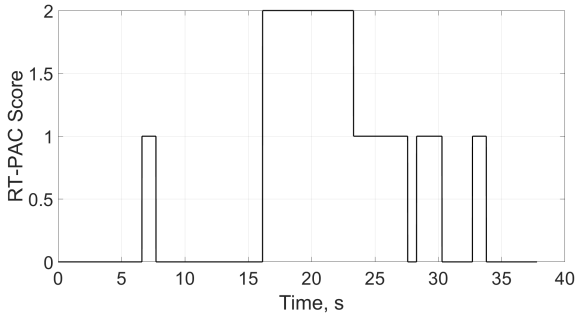

Figure 17. RT-PAC Detection, C4, LR

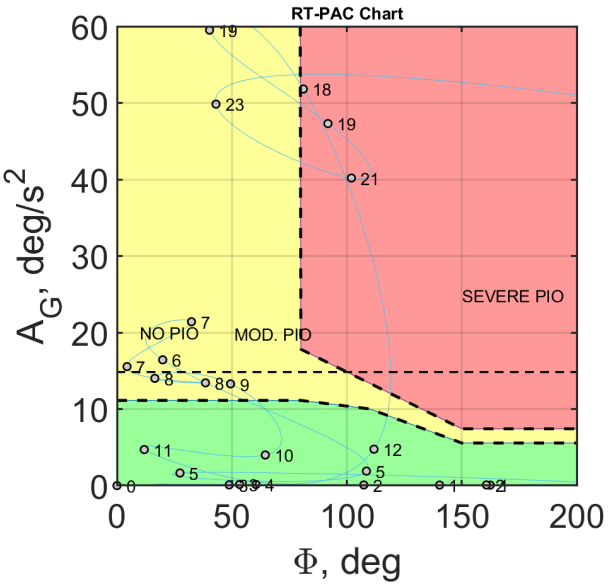

Figure 18. RT-PAC Chart

DISCUSSION

A pilot-in-the-loop experiment was performed to contribute to the development of a real-time PIO detection and warning system. To induce the PVS to enter PIO situations, the baseline rotorcraft configuration was changed with variations of rate limits in the lateral and longitudinal axes. During the tests, a BO105-like rotorcraft dynamics model was used, and the Precision Hover and Lateral Reposition MTEs were chosen. As expected and confirmed by the pilot's subjective ratings, reducing the rate limits leads to a decrease in task performance and induces the PVS to be more PIO prone. This happened quite clearly within the Precision Hover maneuver when moving from C5 to C6, i.e. when changing the longitudinal rate limit from 3.6 deg/s to 1.8 deg/s, while the lateral rate limit was kept at 1.8 deg/s. During the Lateral Reposition maneuver the degradation of performance was already visible for configurations less stringent in terms of rate limits, indicating that the PVS may be more PIO prone during Lateral Reposition than Precision Hover. However, for both MTEs, the variations in configuration led to severe sustained oscillations which required high level of adaptation and consumed the majority of pilot workload.

Thanks to the current experiment, a certain number of data was collected for different rotorcraft configurations, i.e. seven different combinations of lateral and longitudinal rate limits. Looking at the resulting experiment data, it is clear that despite the number of conditions tested, a larger test matrix and more data are needed to obtain more meaningful results. Increasing the number of test pilots would also allow for comparison between pilots and more sensible data.

As for the warning system, the idea was to keep it as simple as possible. One idea to keep the display even simpler, could be to use only one circle indicating the presence of the PIO and then the arrows indicating the axis where the PIO is occurring. But this is probably not the most complete option, because it would not present all the possible PIO information to the pilot, i.e. all the combinations of severity and axis-related PIOs at the same time.

The specific choice of the cues to provide the pilot with, will be the subject of further investigation, which needs pilot advice and further testing. The main advantage of using visual cues with respect to aural cues, is that they easily allow the pilot to be alerted to the PIO real-time detection in both the lateral and longitudinal axes, by immediately showing the PIO severity signal on the head-up display. However, there is a risk that the visual cue could be missed. Other options are Aural and Haptic cues. The intent is to investigate both of these during the project.

CONCLUSIONS AND RECOMMENDATIONS

In this paper, an experiment with a highly qualified test pilot was performed to investigate the feasibility of a real-time PIO detection and warning system, as well as pilot's adaptation and sensitivity to variations in rate limits causing system instabilities during the Precision Hover and Lateral Reposition MTEs. During the trial, objective PAC calculations and subjective pilot ratings were collected for seven different tested rotorcraft configurations, i.e. those given by a combination of the rate limits variation (5, 3.6, 2.5, 1.8 and 1.25 deg/s) in the lateral and longitudinal axes. Overall, the results show a good correlation between objective and subjective evaluations, and that it is possible to detect PIOs in real-time and advise the pilot of the same by means of visual cues. The RT-PAC algorithm does provide useful and timely information as well as providing an indication about the PIO severity. Therefore, this approach shows good potential for the usefulness of a real-time PIO/RPC detection and warning system; nevertheless, since PAC has been developed for a specific kind of rotorcraft and with a limited number of test pilots, its "universal" adaptation to other kinds of rotorcraft and pilots still has to be verified, which means that further research and testing will be needed.

AUTHORS CONTACTS

Simone Fasiello: s.fasiello@liverpool.ac.uk
Michael Jump: mjump1@liverpool.ac.uk
Pierangelo Masarati: pierangelo.masarati@polimi.it

ACKNOWLEDGMENTS

The NITROS project has received funding from the European Union's Horizon 2020 research and innovation program under the Marie Skłodowska-Curie grant agreement No. 721920.

REFERENCES

[1] Anon., "Aviation Safety and Pilot Control: Understanding and Preventing Unfavorable Pilot-Vehicle Interactions," Committee on the Effects of Aircraft-Pilot Coupling on Flight Safety Aeronautics and Space Engineering Board Commission on

Engineering and Technical Systems National Research Council, Washington, D.C., 1997.

[2] D. T. McRuer, "Pilot-Induced Human Oscillations Behavior and Dynamic," NASA Contractor Report, 1995.

[3] M. D. Pavel *et al.*, "Adverse rotorcraft pilot couplings - Past, present and future challenges," *Prog. Aerosp. Sci.*, vol. 62, pp. 1–51, 2013.

[4] M. Jones and M. Jump, "New methods to subjectively and objectively evaluate adverse pilot couplings," *J. Am. Helicopter Soc.*, vol. 60, no. 1, p. 011003, 2015.

[5] M. Jones, "Prediction, Detection, and Observation of Rotorcraft Pilot Couplings," Univeristy of Liverpool, 2015.

[6] D. G. Mitchell and R. H. Hoh, "Development of Methods and Devices to Predict and Prevent Pilot-Induced Oscillations," AFRL-VA-WP-TR-2000-3046, 2000.

[7] D. G. Mitchell, A. J. Arencibia, and S. Muñoz, "Real-time Detection of Pilot-Induced Oscillations," in *Collection of Technical Papers - AIAA Atmospheric Flight Mechanics Conference*, 2004.

[8] D. G. Mitchell and D. H. Klyde, "Identifying a PIO signature - New techniques applied to an old problem," *Collect. Tech. Pap. - 2006 Atmos. Flight Mech. Conf.*, vol. 2, no. August, pp. 992–1006, 2006.

[9] D. DiFranco, "Flight Investigation of Longitudinal Short Period Frequency Requirements and PIO Tendencies," AFFDL-TR-66-163, 1967.

[10] Anon., "MIL-HDBK-1797 - Handbook - Flying Qualities of Piloted Aircraft," Department of Defence, United States of America, 1997.

[11] C. L. Blanken, R. H. Hoh, D. G. Mitchell, and D. L. Key, "Test Guide for ADS-33E-PRF," 2008.

[12] W. R. Gray, "Boundary-avoidance tracking: A new pilot tracking model," in *Society of Flights Test Engineers, SFTE 36th Annual Symposium Proceedings*, 2005.

[13] W. R. Gray, "Handling qualities evaluation at the USAF test pilot school," in *AIAA Atmospheric Flight Mechanics Conference*, 2009.

[14] M. White, P. Perfect, G. Padfield, "Acceptance testing and commissioning of a flight simulator for rotorcraft simulation fidelity research", 2013.

[15] G. E., Cooper, and J. R. P., Harper, "The Use of Pilot Rating in the Evaluation of Aircraft Handling Qualities," NASA TN D5153, 1969.

[16] A. H. Roscoe and A. H. Ellis, "Technical Report TR 90019: A subjective rating scale for assessing pilot workload in flight: A decade of practical use," *Royal Aerospace Establishment*, 1990.